Magnetic Fields of the Radio Frequency Spin Rotator for the NPDGamma Experiment

P.-N. Seo, J.D. Bowman, S.I. Penttila, and W.S. Wilburn

Sept. 3, 2004

1. Introduction

NPDGamma collaboration has been developing a sensitive experiment to measure the parity-violating directional asymmetry of the emitted gamma rays with the neutron spin direction, A_γ, from the $\vec{n}$+p->d+γ reaction. A predicted value of this asymmetry is 5×10^{-8} and the experiment aims to reach a precision of 0.5×10^{-8}. Final statistical uncertainty will depend on the counting statistics of cold neutrons captured in the hydrogen target and thus any systematic error has to be suppressed below this statistical limit [1].

A source of a systematic error produces a signal in a detector that is coherent with the state of the neutron spin. A good example of this type of a source to introduce a false asymmetry is a RF magnetic field used to set the neutron spin state. This field might be coupled to the gamma detector and led a false asymmetry which is larger than the parity-violating asymmetry from the n-p reaction. Sources of systematic errors can be instrumental and are present whether or not neutrons are being detected or they can arise from another polarized neutron interaction besides the n-p capture reaction. The most important experimental tool to isolate a parity-violating signal in the experiment is the neutron spin rotator. Therefore, it is essential that reversing the neutron spin with the spin rotator is well isolated from the rest of the apparatus.

We have measured and calculated magnetic fields of the radio frequency spin rotator that was developed for the NPDGamma experiment to understand its performance such as the spin reversal efficiency and the possible depolarization. With the known fields a reliable model for the experiment can be established to simulate the spin reversal of the neutron spin at different energies.

2. The NPDGamma Spin Flipper

There are a number of techniques, which can be used for reversal of the neutron spin in a beam [2,3,4,5]. Because of the homogeneous 10 G holding field, NPDGamma requires to use a Radio Frequency Spin Rotator (RFSR). This resonance device consists of a solenoid 30 cm in diameter and 30 cm long with its axis along the beam. To shield the rest of the experiment from the RF magnetic fields of the RFSR, the solenoid is mounted into an aluminum cylinder of 40 cm in diameter and 40 cm long. The solenoid is shown in Fig.1 (left) and the aluminum shielding can in Fig.1 (right). The length and the diameter of the solenoid have been optimized for the NPDGamma experiment. The spin rotator has to accept a neutron beam that is defined by a 9.5 cm x 9.5 cm neutron guide of the flight path 12 and the collimation system. The spin rotator must be large enough to efficiently reverse the polarization of this size of a neutron beam. Since the spin reversal takes place adiabatically the length of the RFSR has been selected so that spins of neutrons are effectively reversed up to 100 meV. Once the length of the spin rotator was constrained, the diameter could be optimized. It was found that the diameter to the length ratio of 1:1 was nearly optimum.

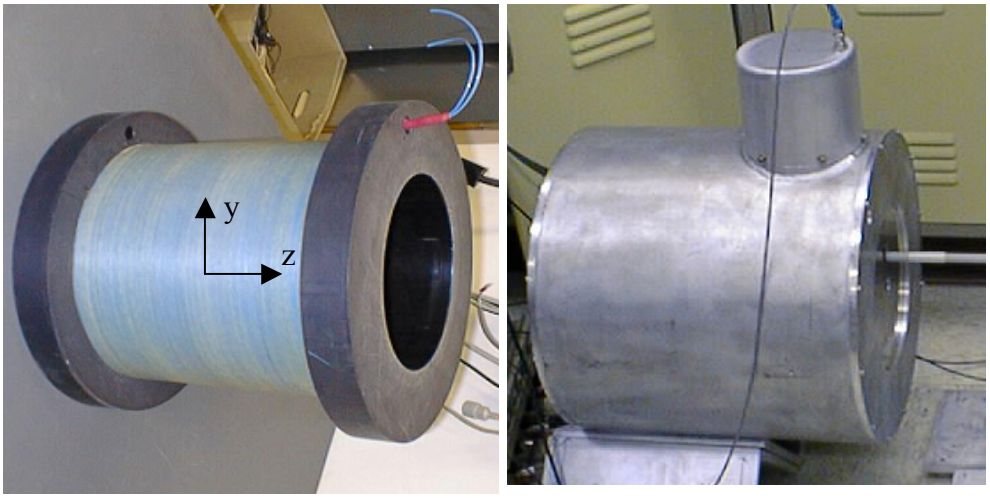

Figure 1. Solenoid of the RF Spin Rotator and its aluminum shielding cylinder.

The cylindrical aluminum shield is larger than the RF solenoid to reduce the transverse gradients at the position of the entrance and exit windows. Large transverse gradients near the windows can lead to substantial depolarization of the neutron beam off axis. The thickness of the aluminum can is 5 mm and that of the windows is 2 mm. Thick aluminum cylinder shields the electronics of the experiment from the RF field of the RFSR. This is essential for the suppression of spin-correlated noise in the electrical coupling which can be the source of a false asymmetry. The 2-mm thick aluminum in neutron entry and exit windows on the end of the aluminum can allow the beam to pass with only slight attenuation (1 %) while still being 4 times the 0.5 mm skin depth for 30 KHz RF magnetic fields. The shielding effectiveness of he 2-mm thick end windows is about 35 dB.

Eighteen gauge (~1.1 mm diameter) Cu wire was wound with 273 turns of a single layer on a nylon spool. The inductance of the solenoid is 8.3 mH and the solenoid becomes a serial circuit with a capacitance that has a resonance frequency of 30 kHz. The capacitance is in the tower on the top of the aluminum cylinder as shown in Fig. 1 (right). The tuned serial resonance circuit has a minimum impedance at resonance that allows to maximize current which is the magnetic strength. The time constant of the resonant circuit is xx μs. The waveform for the spin rotator is created by two HPxxx waveform generators. The first is used to generate the 1/time amplitude modulated waveform and to trigger the amplitude modulation to T_0, a LANSCE accelerator proton beam monitor signal. The second waveform generator is used to provide the nominal 29.6 kHz (the Larmor frequency in a 10 G holding field in y direction) sine wave whose amplitude is modulated by the output of the first waveform generator. The resulting waveform is amplified to provide sufficient current to the spin rotator solenoid.

3. Measurement of Magnetic Fields of the RFSR

In order to scan the magnetic field inside the RFSR, we mounted a small probe coil in a probe housing, two arms to define vertical axis (y-axis) to a holder that was parallel to the spin rotator axis. This probe system was mounted on a scanner. A wire of the probe was enamel-coated Cu and all others components were made of plastic (PVC). Figure 2 shows this setup for the field measurement.

First, we leveled the aluminum can and the spool of the solenoid. Then, we lined up the spool and the can with a laser beam. Then, the scanner on which the probe housing with the probe, the rotational arm, and the supporting arm were mounted was leveled and lined up with the spin rotator. We carefully centered the center of the probe to the axis of the spin rotator. In order to measure B_z and B_r off axis components, we cut a small hole off the front Al window of the spin rotator as shown in Fig. 2. During measurement the hole was covered by an aluminum pieces.

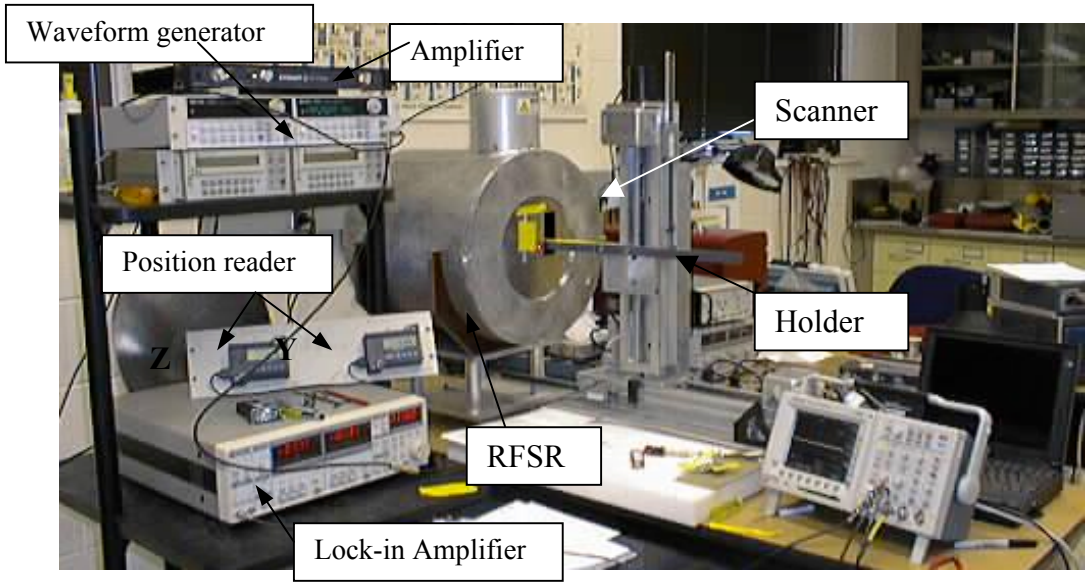

Figure 2. Setup of the field measurement of the RFSR. The probe and two arms are mounted on the holder. The holder is attached to the scanner. The 30 kHz RF field was generated by the waveform generator and was amplified. The RFSR signals from the probe was monitored with a scope and measured with a Lock-in amplifier.

A 100 mV_{PP} (corresponding to 1 Amp current) sine wave at 28.99 kHz from the waveform generator was sent to a Lock-in amplifier as a reference and to an audio amplifier for amplification and the output of the audio amplifier was sent to the serial tuned LC resonance circuit where L is the inductance of the solenoid. Outputs voltage of the probe coil was sent to the Lock-in amplifier as an input. Root-mean-squared output voltage of the Lock-in amplifier was converted into the strength of the measured magnetic field.

The probe to measure the RF fields was simply 16 turns of coiled wire with 7.8 mm diameter. In Fig. 3 (a), the probe for the radial field component (B_r) measurement was pivoted

with the rotational arm and the holder. Figure 3 (b) shows how the supporting arm and the rotational arm worked to turn the axis of the radial field perpendicular to the spin rotator axis. When a screw rotated, the radial field probe rotated either toward the supporting arm or to an opposite direction. Since the radial field (B_r) is much smaller than the axial field (B_z), it could be easily contaminated by the axial field and it was very important to make sure that the axis of the radial field probe was perpendicular to the spin rotator axis. For the same reason, the coil of the probe was carefully wound so that every wound was perpendicular to the axis of the coil. To measure B_z, the probe shown in Fig. 3 (a, b) was rotated by 90 degrees as shown in Fig. 3 (c) without changing the pivot point.

We scanned from the back window of the RFSR by 10-mm step on and off z-axis as far as the scanner reaches the limit in the direction. We measured the field, B_z, at r=0, 2.5, and 5 cm and the field, B_r, at r=0, -0.78, 2.5, and 5 cm. The measured fields as a function of z are shown in Fig. 4. Maximum B_z field on axis is 4.22 G at the center of the spin rotator and B_z fields are increased as r is closed to the boundary of the aluminum cylinder. The field was increased, as it was closer to the boundary of the can. On the axis, B_r=0 and the off axis B_r fields increase near the ends of the solenoid.

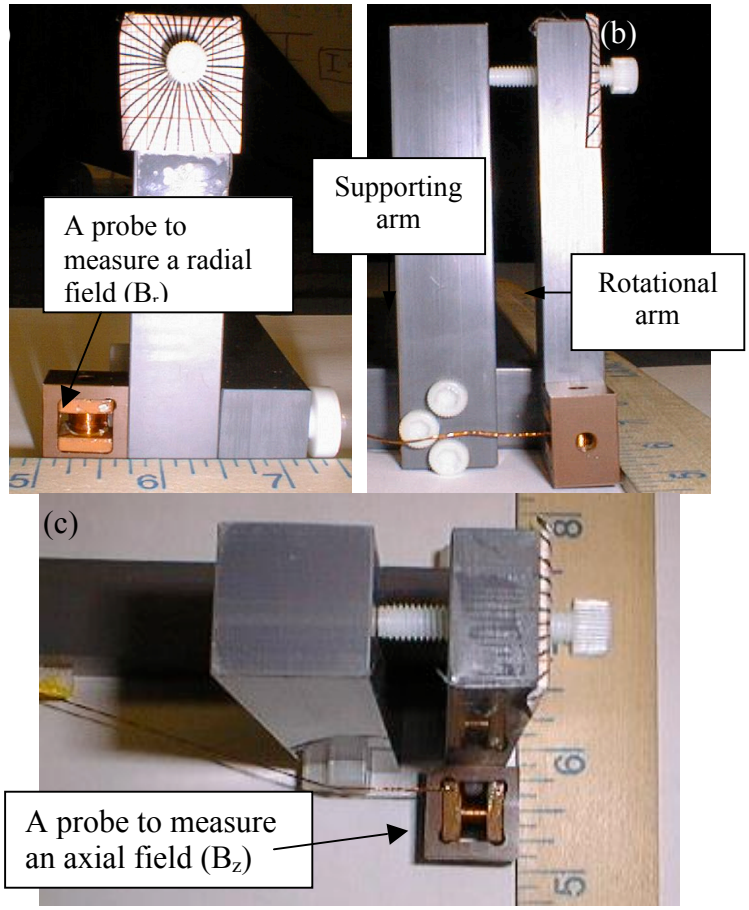

Figure 3. The probe coil to measure the magnetic fields of the RFSR: (a) the radial field probe is pivoted with the rotational arm to the holder, (b) the rotational arm and the supporting arm, and (c) the axial probe.

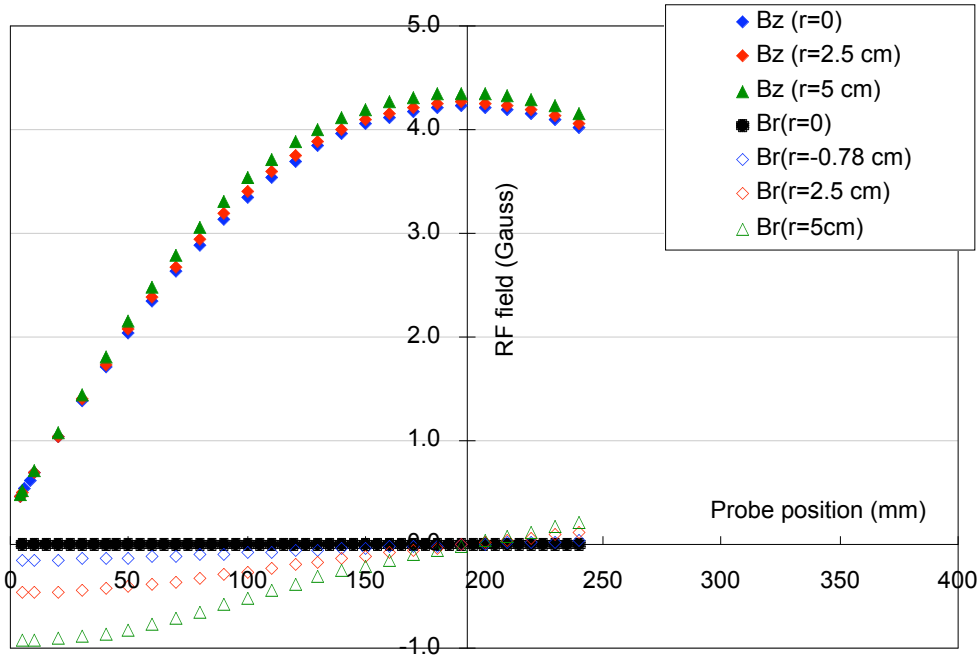

Figure 4. Results of mapping B_z and B_r fields of the spin flipper on axis and off axis.

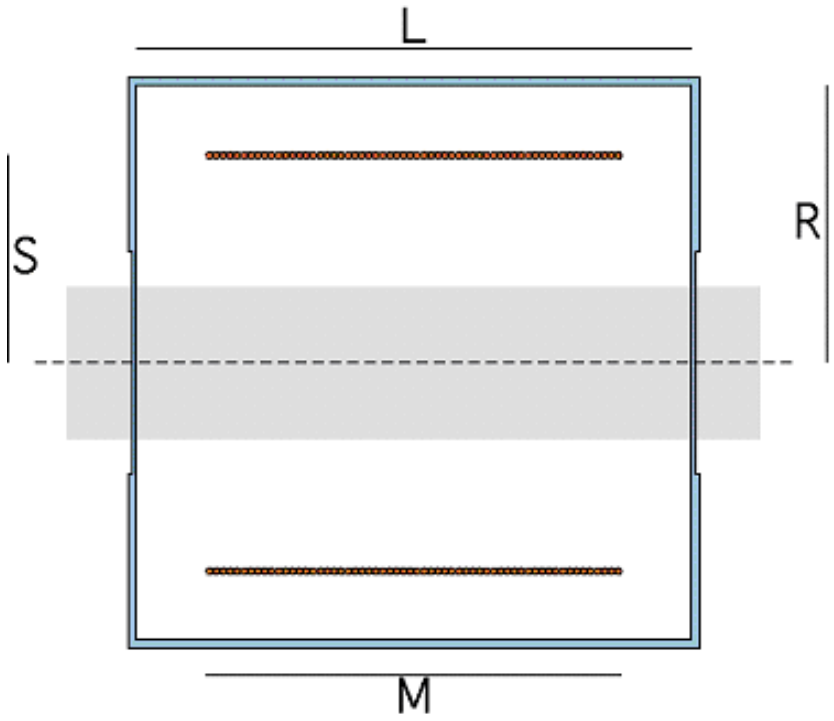

Figure. 5. Approximate scale drawing of the radio frequency spin flipper. The RFSR is a figure of rotation about the dashed line. The (blue) aluminum body of the RFSR is a right circular cylinder. The dimensions are L=40 cm, M=30 cm, R=20 cm, and S=15 cm. The guide field is vertical, y, and the neutrons move horizontally, z. The gray region is the extent of the neutron beam.

4. Calculation of Magnetic Field of the RFSR

The magnetic field inside the cylinder is calculated as the gradient of a potential, $\varphi(r,z)$. The wavelength (λ, several kilometers) of the 28.99 kHz electric and magnetic field is large compared to the dimensions of the RFSR. We calculated the field neglecting retardation effects.

The skin depth (0.5 mm) in the aluminum cylinder is small compared to the dimensions of the cylinder. We approximate the effects of the eddy currents in the aluminum cylinder by imposing the boundary conditions that the component of the magnetic field normal to the surfaces of the cylinder vanishes. The fields are cylindrically symmetric. In a cylindrical coordinate system with the z-axis as shown in Fig. 5, the axis of symmetry the dashed line, the potential does not depend on the azimuthal angle. We separate variables and seek solutions of the form $\varphi(r,z) = f_n(r)g_n(z)$. The solutions are

$$f_n(r) = I_0(k_n r) \text{ or } f_n(r) = K_0(k_n r)$$
$$g_n(z) = sin(k_n z) \text{ or } g_n(z) = cos(k_n z).$$

We divide the interior of the cylinder into two regions, one inside the solenoid and one outside the solenoid. Because the magnetic field is regular at $r = 0$, the coefficient of the $K_0(k_n r)$ term vanishes. The field must be an even function of z; hence the coefficient of the $cos(k_n r)$ term vanishes in both regions. We impose the boundary condition at the ends of the cylinder, $z = \pm L/2$; the z component of the field vanishes, $B_z(r,L/2) = 0$, hence $k_n = (2n-1)\pi/L$. We can therefore write the potential as a sum over *n*

$$\varphi_{inner}(r,z) = \sum_{n=1}^{\infty} \alpha_n I_0(k_n r) sin(k_n z),$$
$$\varphi_{outter}(r,z) = \sum_{n=1}^{\infty} sin(k_n r)\left(\beta_n I_0(k_n r) + \gamma_n K_0(k_n r)\right).$$

We impose two boundary conditions at $r = S$, $B_r(S,z)$ must be continuous, and at $r = R$, $B_r(R,z) = 0$. These two boundary determine β_n and γ_n assuming α_n to be known. The boundary condition $\frac{d}{dz}\left(\varphi_{outer}(S,z) - \varphi_{inner}(S,z)\right) = J$, where J is the surface current density in the solenoid, then determines the α_n by using the orthogonal of the $g_n(z)$.

$$J \int_{-M/2}^{+M/2} cos(k_n z)dz = k_n \int_{-L/2}^{+L/2} cos^2(k_n z)\left((\beta_n - \alpha_n)I_0(k_n S) + \gamma_n K_0(k_n S)\right) \text{ or}$$
$$\frac{2J\, sin(k_n M/2)}{k_n} = \frac{k_n L}{2}\left((\beta_n - \alpha_n)I_0(k_n S) + \gamma_n K_0(k_n S)\right).$$

We calculated the fields as a sum of the first 40 terms of the infinite series. The *z* and *r* components of the field are shown in Figs. 6 and 7. In Fig. 8, we compare measured fields with

calculated fields of B_z at r=0 and B_r at r=5 cm. Data were shifted by 8 mm towards the back window because the center of the probe was 8 mm off from the back window due to protruding the rotating screw shown in Fig. 2.

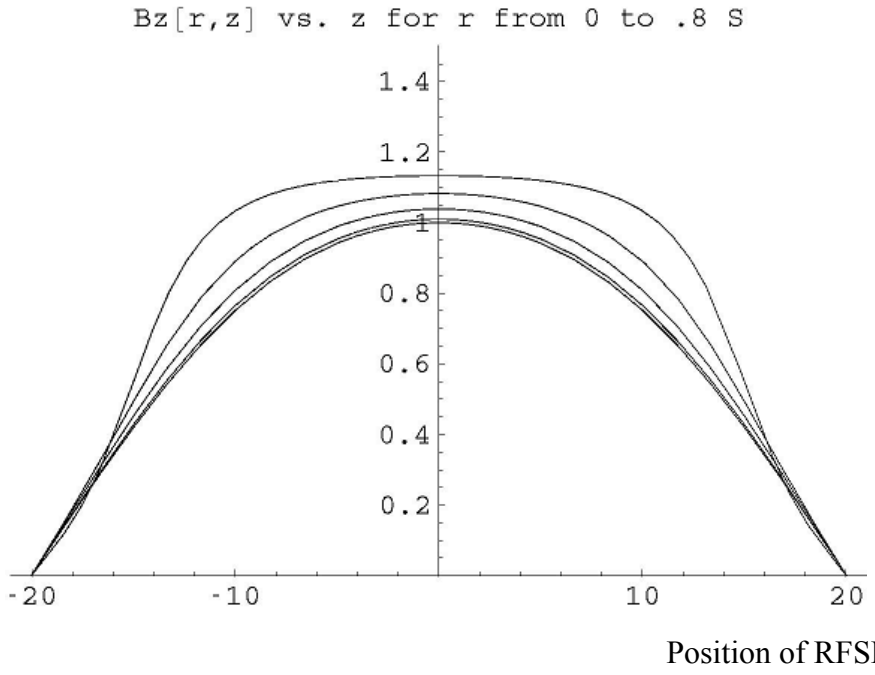

Figure 6. $B_z(r,z)$ as a function of z for $r = 0, .2, .4, .6,$ and $.8\ S$. The field increases as r increases.

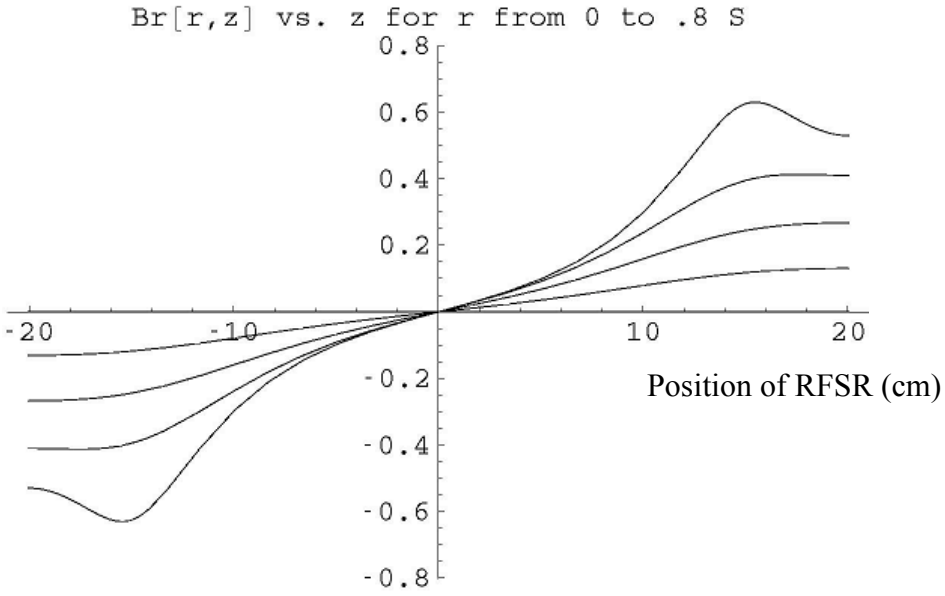

Figure 7. $B_r(r,z)$ as a function of z for $r = 0, .2, .4, .6,$ and $.8\ S$. The field is small for small r or z. Near the ends of the solenoid, the radial component of the field increases.

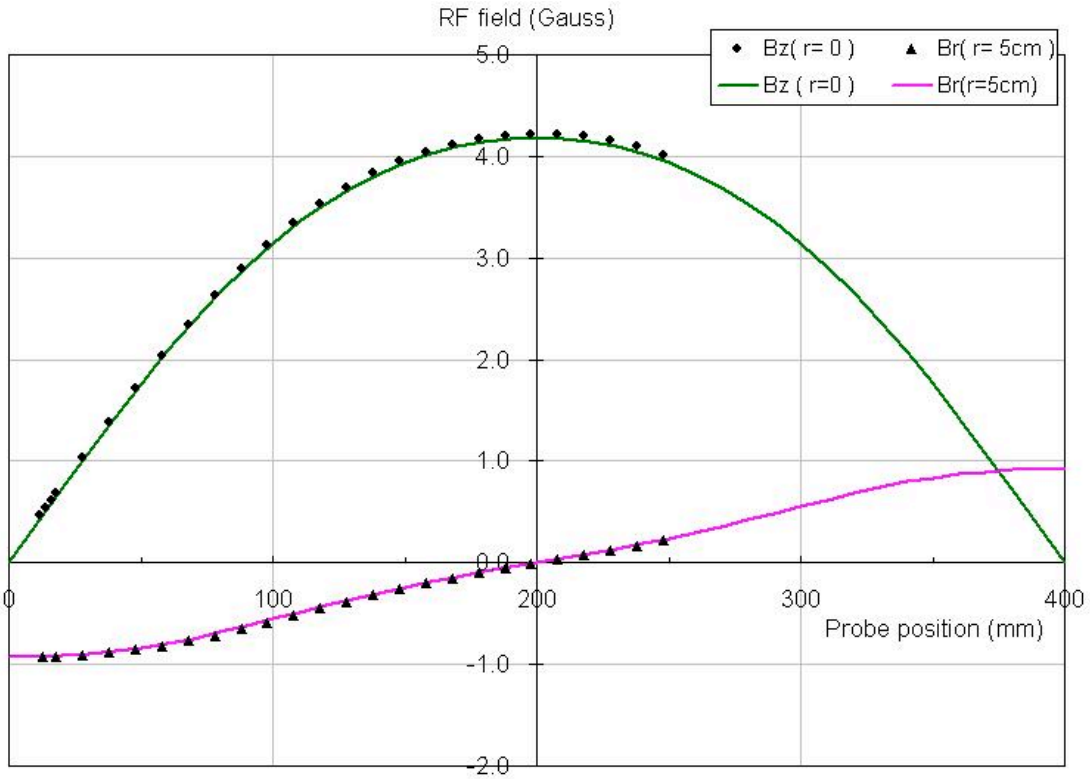

Figure 8. Comparison of measured fields (circle and triangle) and calculated fields (solid line) at $B_z(r,z)$ at r=0 and $B_r(r,z)$ r=5 cm inside the RFSR.

5. Conclusion

We have measured and calculated the magnetic field of the RFSR, which was developed for the NPDGamma experiment. As expected, results show that the axial field has maximum at the center of the spin rotator and the strength of the off-axis radial field increase towards near the ends of the spin rotator. Measured fields are compared with calculated fields and they agree well. The aluminum end windows of the shielding cylinder do not disturb much the field.

References

[1] W.M. Snow et al., Nucl. Inst. and Meth. A 440(2000) 729
[2] L.W. Alvarez and F. Bloch, Phys. Rev. 57 (1940) 111
[3] G.M. Drabkin, JETP 43 (1962) 1107
[4] F. Mezei, Z. Physik 255 (1972) 146
[5] A.I. Egorov, V.M. Lobashev, V.A. Nazarenko, G.D. Porsev, and A.P. Serebrov, Sov. J. Nucl. Phys. 19 (1974) 147